REPORT DOCUMENTATION PAGE

FORM APPROVED
OMB No. 0704-0188

1. AGENCY USE ONLY (Leave blank)	2. REPORT DATE	3. REPORT TYPE AND DATES COVERED
	09/19/96	Final Technical Report/1993-1996

4. TITLE AND SUBTITLE OF REPORT
Property Control of (Perfluorinated Ionomer)/(Inorganic Oxide) Composites by Tailoring the Nanoscale Morphology

5. FUNDING NUMBERS
Grant Number:
AFOSR FY9620-93-1-0189 DEF
61102F
2303/CS

6. AUTHOR(S)
Kenneth A. Maurtiz, Robert B. Moore

7. PERFORMING ORGANIZATION NAME(S) AND ADDRESS(ES)
Department of Polymer Science
Box 10076
University of Southern Mississippi
Hattiesburg, MS 39406-0076

AFOSR-TR-96
0456

9. SPONSORING/MONITORING AGENCY NAME(S) AND ADDRESS(ES)
Air Force Office of Scientific Research (AFOSR/PKA)
110 Duncan Avenue, Suite B115
Bolling Air Force Base, D.C. 20332-0001
NE
Lee

10. SPONSORING/MONITORING AGENCY REPORT NUMBER:

11. SUPPLEMENTARY NOTES:

12a. DISTRIBUTION AVAILABILITY STATEMENT
Approved for public release;
distribution unlimited.

12b. DISTRIBUTION CODE

13. ABSTRACT (Maximum 200 words)

The morphology and properties of perfluorosulfonate ionomers (PFSI's) can be significantly altered by simple changes in the type of counterion used to neutralize the membrane. Furthermore, with a range of counterions, different solution and melt-processing procedures may be used to control the size and shapes of the ionic domains in PFSIs. A major objective of this research was to test our hypothesis that nanophase-separated morphologies of PFSIs act as catalytic templates that control the morphology of in situ-grown, sol-gel derived phases. This hypothesis was verified for PFSI/[SiO_2] and PFSI/[organically-modified SiO_2] hybrids using SAXS. Nanostructures based on the alkoxides of Si, Ti, Al, Zr and alkylalkoxysilanes were probed by various spectroscopic and x-ray scattering methods. The mechanical, thermal and degradative properties of these hybrids can be engineered via nanostructural manipulation. Two forms of compositional gradients were generated within PFSIs: (1) SiO_2 nanoparticle *cores* having organic or metal oxide *shells*; (2) gradients of inorganic composition across film thicknesses. Gas permeation and liquid sorption can be manipulated via nanostructural tailoring as well as by composition gradients. PFSI SO_2F precursors can be cross linked and inorganic phases introduced via in situ amination and sol-gel reactions for aminopropyltriethoxysilane.

19961016 097

14. SUBJECT TERMS

DTIC QUALITY INSPECTED 4

15. NUMBER OF PAGES:

16. PRICE CODE

17. SECURITY CLASSIFICATION OF REPORT:	18. SECURITY CLASSIFICATION OF THIS PAGE	19. SECURITY CLASSIFICATION OF ABSTRACT	20. LIMITATION OF ABSTRACT
U	U	U	U

23 SEP 1996

Final Technical Report
Project Title:

Property Control of (Perfluorinated Ionomer)/(Inorganic Oxide) Composites by Tailoring the Nanoscale Morphology

Kenneth A. Mauritz and Robert B. Moore
Department of Polymer Science
University of Southern Mississippi
Hattiesburg, MS 39406

AFOSR GRANT AWARD # AFOSR FY9620-93-1-0189 DEF

TABLE OF CONTENTS

C. TGA-FTIR Investigation of the Thermal Degradation of Nafion®/[Silicon Oxide] Nanocomposites

D. Chemical Modification of a Nafion® Sulfonyl Fluoride Precursor via *in situ* Sol-Gel Reactions

E. [Perfluorosulfonate Ionomer]/[(Silicon + Metal) Oxide] Nanocomposites *via* Polymer - *in situ* Sol-Gel Chemistry

1. Nafion®/[(*mixed* SiO_2-TiO_2) and (*mixed* SiO_2-Al_2O_3)] Nanocomposite Films

2. Nafion®/[SiO_2-TiO_2] Nanocomposite Films: Sequential Alkoxide Procedure

F. Asymmetric Nafion®/[Zirconium Oxide] Hybrid Films via *in situ* Sol-Gel Chemistry

G. Base-Catalyzed Sol-Gel Reactions of TEOS within the Nanophase-Separated Morphology of Nafion® Membranes

IV. Refereed Journal Publications Resulting from this Work

V. Students and Postdoctorals Involved in this Work

IV. Projected Applications

I. INTRODUCTION

The nanocomposite component of this work proceeded under the following assumptions: (1) The nanometers-in-size polar clusters that are dispersed throughout Nafion® membranes would be domains in which sorbed silicon alkoxides, metal alkoxides, alkylalkoxysilanes, or mixtures of these monomers, would preferentially reside; (2) the hydrolysis-condensation polymerization of these monomers will be initiated in hydrated clusters and catalyzed via pendant $-SO_3H$ and $-SO_3^-X^{+z}$ groups; (3) the quasi-ordered array of clusters would act as a 3-D template that directs the morphology of the dried filler phase. Guided by these working hypotheses, an array of nanocomposite membranes, consisting of Nafion® possessing silicate, organically-modified silicate, titanate, silicate-titanate, silicate-aluminate and zirconate nanophases were formulated and evaluated for structure on a number of scales and a large number of properties as described in the narrative. At the end of this report, we suggest a number of significant applications for these unique hybrid materials.

The concluded effort summarized in this report was jointly funded by grants from the Air Force Office of Scientific Research, Air Force Systems Command (AFOSR F49620-93-1-0189), administered through Program Director Dr. Charles Y.-C. Lee, and the National Science Foundation (Advanced Polymeric Materials: DMR-9211963)/Electric Power Research Institute, administered by Program Director, Dr. Norbert Bikales.

II. TAILORING THE MORPHOLOGY-PROPERTY RELATIONSHIPS IN PERFLUOROSULFONATE IONOMERS

A study was performed that examined the barriers to flow in semicrystalline perfluorosulfonate ionomers (PFSIs). It was found that the most significant barriers to flow in PFSIs are polymer crystallinity and strong electrostatic crosslinks. The "PTFE-like" crystallinity was removed by evaporation of the ionomer solutions, and the electrostatic crosslinks were weakened by neutralizing the ionomer with large, hydrophobic tetrabutylammonium counterions. To yield the desirable melt-flow properties, the bulky counterions function as internal plasticizers and form weak ion pair dipoles which diminish the attractive forces responsible for ionic aggregation.

In order to better understand how the tetrabutylammonium counterions weaken ionic aggregation, an investigation into the effects of hydrophilic and hydrophobic counterions on the Coulombic interactions in PFSIs was performed.

In this study attenuated total reflectance FTIR spectroscopy was used to compare the influence of hydrophilic and hydrophobic counterions on the vibrational behavior of the sulfonate and perfluoroether groups in 1100 equivalent weight (EW) Nafion® and 803 EW Dow perfluorosulfonate ionomer membranes. For dry, Na^+ -form membranes, the infrared band attributed to the $—SO_3^-$ symmetric stretching vibration was found to shift to higher frequencies

with an increase in the degree of neutralization. In contrast, neutralization with tetrabutylammonium ions caused the $— SO_3^-$ vibrational band to shift to lower frequencies with increasing neutralization. This behavior was attributed to a diminished polarization of the $— SO_3^-$ groups by the hydrophilic and diffusely charged TBA^+ cations, relative to the strong polarization observed with Na^+ ions. Vibrational bands attributed to perfluoroether groups in close proximity to the sulfonate groups were also found to be influenced by Coulombic interactions within the clusters. The frequency shifts of these bands followed a trend that was virtually identical to that observed for the $— SO_3^-$ symmetric stretch. This behavior was attributed to a combination of through-space, dipolar field effects, and through-bond inductive effects, from the neighboring ionic groups. In Nafion®, the ether groups directly attached to the backbone are shielded from the Coulombic interactions within the clusters, while the ether groups within three bonds of the terminal ionic groups are very sensitive to the state of polarization of the sulfonate anion. Thus, small inorganic ions form strong electrostatic dipoles, which upon ionic aggregation yield strong electrostatic crosslinks. In contrast, the relatively large size and diffuse ionic charge of the $— SO_3^-TBA^+$ ion pairs generates weak Coulombic interactions and thus weak electrostatic crosslinks. Therefore, the melt-flow properties of PFSIs are governed by the strength of Coulombic interactions.

The dramatic plasticization by TBA^+ counterions permitted PFSIs to undergo considerable deformation. Thus, the effect of uniaxial orientatin on the structure and properties of Nafion® PFSI was examined. Anisotropic, 2-dimensional small- and wide-angle X-ray scattering data showed that uniaxial extension of perfluorosulfonate ionomers containing tetrabutylammonium ions creates an oriented morphology that persists after the samples are isolated from the extensional stress. Upon conversion of the oriented ionomers to the ionically conductive sodium form, surface measurements showed that ionic conductivity along the direction of uniaxial orientation was 40% greater than along the perpendicular direction.

Because the TBA^+ counterions was so effective in altering the physical properties of PFSIs, studies were carried out on the effects of alkylammonium counterion size on PFSI physical properties. Dynamic mechanical studies were performed on Nafion® and Dow PFSIs containing a variety of alkylammonium counterions. As the counterion size increased, relaxations associated with the ionic aggregates and polymer matrix were systematically shifted to lower temperatures. The temperature at which long range chain slippage (flow) occurred was lowered with increasing counterion size.

A. Effect of Counterion on the Physical Properties of Perfluorosulfonate Ionomers

The physical properties of ionomers can be significantly altered by the type of counterion used for neutralization. Though metal counterions have been shown to form very strong ionic aggregates in the dry state, the latitude in polymer physical properties that can be gained by changing the type of metal counterion is somewhat limited. In general, the larger and more diffusely charged the counterion, the less effective it is at crosslinking. Compared to the alkali

metal counterions, ionomer properties can be varied significantly by neutralization with organic counterions, such as with the alkyl amines.[1,2,3]

Studies involving ionomers containing alkyl amines have demonstrated that the amines function as plasticizers.[1,2,3] This plasticization was found to increase with increasing alkyl chain length on the amine. These studies point out the utility of using organic counterions to tailor the physical properties in ionomer systems. As an added advantage, the organic counterions are bound through ionic interactions to the polymer chain, and are less likely to diffuse out of the polymer, as is typical with more commonly used plasticizers.[2]

It was previously shown that tetrabutylammonium (TBA^+) neutralized Nafion® exhibited enhanced melt-flow properties. Dynamic mechanical studies of the TBA^+-form Nafion® revealed that the relaxations attributed to the ionic aggregates and the matrix were lowered in temperature by as much as ca. 150 °C compared to the same relaxations in the sodium (Na^+) neutralized materials.[4] The large TBA^+ counterions function as effective internal plasticizers and form weak ion pair dipoles which diminish the attractive forces for ionic aggregation. Thus, the ability to manipulate the morphology in Nafion® PFSIs is greatly enhanced by using TBA^+ counterions. The work done with uniaxially oriented Nafion® materials[5] is an excellent example of the improved control of ionomer properties gained through counterion manipulation.

The research described thus far has dealt only with the TBA^+ counterion. To date, no systematic evaluation of alkylammonium counterion size on the thermomechanical properties of PFSIs has been performed. Therefore, in light of the previous work done on alkyl amine containing hydrocarbon ionomers, this work examines the effects of alkylammonium counterions on the properties of PFSIs. The short side chain Dow ionomers have been included for comparison purposes.

Experimental

Materials

Nafion® 117 (1100 EW, sulfonic acid form) was obtained from E. I. DuPont de Nemours & Co. Dow PFSI membranes (H^+-form), having equivalent weights EW of 803 and 1000 g/mole, were obtained from the Dow Chemical Company. The tetra-methyl (TMA^+), ethyl (TEA^+), propyl (TPA^+), and butylammonium (TBA^+) counterions were obtained from Aldrich in the form of hydroxides dissolved in either methanol or water. The tetra-pentyl ($TPentA^+$), hexyl ($THexA^+$), heptyl ($THepA^+$), octyl ($TOctA^+$), and decylammonium ($TDecA^+$) counterions were obtained from Aldrich as bromide salts. All other reagents were obtained from Aldrich and used without further purification.

PFSI Sample Preparation

All PFSI membranes were precleaned by refluxing in 8M HNO_3 for ca. 12 hrs. These H^+-form membranes were then washed with deionized (DI) water to remove excess acid. A portion of the H^+-form Nafion was converted to the Na^+-form, for subsequent dissolution. Conversion to the Na^+-form was accomplished by first soaking the membranes in an aqueous solution of NaOH and then rinsing the membranes with DI water.

For experiments involving as-received membranes (Nafion® and Dow) neutralized with either TMA^+, TEA^+, TPA^+, or TBA^+ counterions, the membranes were prepared by soaking the H^+-form membranes in an excess (ca. 5X) methanolic solution of the appropriate alkylammonium hydroxide. The neutralized membranes were thoroughly rinsed of excess alkylammonium hydroxide and dried in a vacuum oven at 60 °C overnight.

For experiments involving compression molded Nafion,® the PFSI was stoichiometrically neutralized with one of the 9 alkylammonium counterions. Material preparation consisted of adding a stoichiometric amount of either one of the alkylammonium hydroxides to a H^+-form Nafion® solution, or one of the alkylammonium bromides to a Na^+-form Nafion® solution. The H^+ and Na^+ -form Nafion® solutions were prepared by dissolving the respective membranes in a mixed solvent of 50% DI water and 50% ethanol in a Parr high-pressure reactor at 250 °C with constant stirring, for one hour. The alkylammonium-form Nafion® solutions were allowed to stand overnight, and the solvent was evaporated off. The resultant powders were soaked and rinsed ca. 5 times with large amounts of DI water to remove any NaI salt. The alkylammonium powders were dried in a vacuum oven at ca. 60 °C overnight. Membranes were pressed on a Carver lab press at temperatures that were ca. 20° C above the respective ionic relaxation temperatures.

Analysis

Dynamic mechanical measurements were performed using a Seiko Instruments SDM 5600 Series dynamic mechanical spectrometer (DMS 200). Samples were analyzed in the tensile mode at a frequency of 1 Hz and a heating rate of 5 °C/min.

SAXS data were obtained using a Siemens XPD-700P polymer diffraction system equipped with a two-dimensional, position-sensitive area detector. The sample-to-detector distance was 49 cm. All samples were freestanding, and data were collected in the transmission mode. Corrections were made for background, sample thickness, and absorption.

Results and Discussion

I. Effect of Alkylammonium Counterion Size on the Dynamic Mechanical Properties of Nafion 1100 EW PFSI

Figure 1 shows Tan δ plots for compression molded 1100 EW Nafion®, stoichiometrically neutralized with either TMA^+, TEA^+, TPA^+, TBA^+, $TPentA^+$, $THexA^+$, $THepA^+$, $TOctA^+$, or $TDecA^+$ counterions; the size of the alkylammonium counterions increases from (a)→(i). Two relaxations above 0 °C are clearly evident in the plots. The α peak (i.e., higher temperature peak) has been attributed to relaxations associated with the ionic aggregate, while the β peak (i.e., lower temperature peak) has been attributed to relaxations associated with the matrix.[6] These plots show that both α and β relaxations shift to lower temperature with increasing counterion size, which is consistent with previous observations made on the alkylamine neutralized polystyrene ionomers.[1,2] In contrast to the alkylammonium neutralized PFSIs, Figure 2 shows that changing alkali metal counterions has only a very small influence on the α and β relaxations. The alkali metal counterions form very strong ionic aggregates in the dry state.

A plot of the α and β peak temperatures versus the number of carbons in the alkylammonium groups is shown in Figure 3. From this plot, it is evident that the matrix relaxation undergoes a relatively monotonic depression with increased alkyl chain length. This type of trend has also been observed by Smith et al.[2], who found that the matrix T_g decreased linearly with the number of carbon atoms in the alkyl amine chain. Also, Gauthier et al.[7] found that for alkyated polystyrene-based ionomers, increasing alkylation caused a decrease both the matrix and cluster T_g's. The observed trend is quite reasonable considering that the weight fraction of the counterions increases with increasing counterion size. The bulky counterions reduce the driving force for ionic aggregation, thus the number of lone pairs in the matrix increases. As the number, and size, of lone ion pairs in the matrix increases, there is an increase in the free volume, and a reduction in the matrix T_g.

In comparison to the β relaxation, the response of the α relaxation is nonlinear. Since the α peak has been attributed to relaxations associated with the ionic aggregates, and the bulky counterions would necessarily reside within the aggregates, it is reasonable to expect that this relaxation would be more intimately associated with changes in counterion. Electrostatic interactions and plasticization by alkyl chains are critical factors in ionic aggregate stability.

Data from SAXS experiments show that the ionic aggregate Bragg spacing for TMA^+, $TPentA^+$, and $TDecA^+$ neutralized Nafion® form PFSIs is 32.7, 33.9, and 36.7 Å, respectively. The difference in Bragg spacing is only 4 Å between the extremes in alkylammonium counterion size, suggesting that ionic aggregate dimensions are not increasing substantially with increased counterion size. As discussed, this phenomena could be caused by the ionic groups having a decreased tendency to aggregate, resulting in fewer ion pairs per aggregate. These smaller, weaker aggregates would be less thermally stable, and exhibit a lower relaxation temperature.

Figure 4 shows plots of storage modulus for TMA^+, TEA^+, TPA^+, $TPentA^+$, $THexA^+$, $TOctA^+$, and $TDecA^+$ neutralized Nafion® PFSIs. As the size of the counterion increases, a depression of the modulus over the entire temperature range is observable. The most significant effect of counterion can be seen in the rubbery modulus, and in the terminal region. In addition, the width of the glassy to rubbery transition zone increases with increasing alkylammonium counterion size. Gauthier et al. observed the same phenomena in the alkylated polystyrene-based ionomers, and explained this as a reduction in
the intermolecular interactions, and the destruction of the three-dimensional torsional oscillator lattice.[7] The depression of the rubbery modulus with increasing counterion size, may be attributed to a decrease in the crosslink density.

In the terminal region, bulky counterions can be seen to effectively plasticize the PFSI, shifting the temperature at which long range polymer flow takes place to lower temperatures. This is in agreement with Weiss et al., who observed that the melt index of alkylamine neutralized polystyrene ionomers increased with the bulkiness of the counterion.[1] This phenomena is also seen with the alkali metal neutralized PFSIs (Figure 5), but only to a very slight extent.

It is important to note that thermal stability of alkylammonium counterions in Nafion® has been related to the strength of the sulfonate-counterion interactions.[8] As Figure 6 shows, the PFSI degradation temperature does decrease with increasing counterion size. It is apparent that the initial decomposition temperature decreases with increasing counterion size, which would

indicate that the counterion binding is weaker with increasing size. A decrease in counterion binding helps in explaining the thermomechanical data.

2. Effect of Alkylammonium Counterion Size on the Dynamic Mechanical Properties of Dow 803 and 1000 EW PFSI

Dow ionomers have a shorter side chain than the Nafion® PFSIs. Because of this difference in side chain length, there should be inherent differences in the relaxations in the Dow ionomers compared to the Nafion® PFSIs. Figure 7a and 7b show Tan δ plots for as-received 803 and 1000 EW Dow ionomer containing TMA^+, TEA^+, TPA^+, and TBA^+ counterions. Note that unlike Nafion®, α and β relaxations are barely discernible in the 803 EW PFSI, and completely overlap in the 1000 EW PFSI. This phenomena may be attributed to the closer proximity of the ionic groups to the backbone, which would more closely couple aggregate and matrix relaxations. For the TEA^+, TPA^+, and TBA^+ counterions the relaxations in the 803 EW PFSI occur at slightly lower temperatures than in the 1000 EW PFSI indicating that the greater content of alkylammonium counterion in the 803 EW PFSI causes a greater plasticization effect. The TMA^+ counterion, however, increases the α relaxation with increasing ion content. Weiss et al. have shown that the trimethylammonium counterions increase the T_g of polystyrene ionomers with increasing ion content.[1]

The plasticization of the Dow PFSIs is further illustrated in the storage modulus plots Figure 8a and 8b. Note that the modulus for the 803 EW ionomer drops more for the tetraethyl, tetrapropyl, and tetrabutyl than in the 1000 EW ionomer. Again, the TMA^+ counterion is small enough to permit strong ionic interactions which would tend to raise T_g with increasing counterion content.

Conclusions

This study demonstrates that the type of neutralizing counterion has a dramatic impact on the thermomechanical properties in PFSIs. The alkylammonium counterions effectively plasticize the PFSI, reducing the strength of the ionic aggregates and lower the matrix T_g. By varying the size of the alkylammonium counterion, a broad spectrum of thermal, mechanical, and rheological behavior may be achieved.

B. Solid-State ^{19}F NMR Spectroscopy of PFSIs

^{19}F NMR spectroscopy has proven useful in probing molecular motions in PFSIs.[9,10,11] Boyle et al. have been able to correlate ^{19}F T_1, T_2 and $T_{1\rho}$ data with dielectric and mechanical relaxation experiments on Nafion®. In addition, Schlick et al.[11] performed variable temperature ^{19}F NMR experiments on H^+-form Nafion® PFSI and have associated discontinuities in the spectral line widths, as a function of temperature, to endotherms observed in DSC studies of H^+-Nafion.

Advances in high-speed magic-angle spinning (MAS) NMR spectroscopy has made high resolution ^{19}F spectra of fluorocarbon polymers readily available.[12] High-speed MAS spectroscopy provides new opportunities in probing the complex morphology of PFSIs.

Experimental

Preliminary, variable temperature ^{19}F MAS data was recorded on a Bruker Instruments DMX-400, with a sample spinning rate of 18.7 kHz. Experiments were performed on as-received H^+-form, TPA^+-form, and TBA^+-form Nafion® (1100 EW). Spectra were recorded at 27, 60, 90, 120, and 150 °C.

Results and Discussion

Figure 9 shows the room temperature spectra for H^+-form Nafion®. Spectral assignments are based on previous work by Schlick and coworkers.[11] The unassigned peaks are attributed to side bands and are observed to shift with a change in rotor speed.

Figure 10 shows plots of the full line width, at half-height, versus temperature for the four spectral peaks from Figure 9. The data from the H^+-form, TPA^+-form, and TBA^+-form PFSIs are plotted on each graph. While these data are preliminary, with a paucity of data points, some potentially useful information may be gathered. It is evident that the slopes of the plots for fluorine in the side chains (graphs A,C,D) are steeper than for the backbone fluorine (graph B). This may be attributed to increased mobility of the side chains, over the backbone, with increasing temperature. Of further significance, is the prominent discontinuity in the plot of the H^+-form (graph C). This discontinuity occurs over a temperature range in which mechanical relaxations, attributed to the ionic aggregates, have been observed. While it is apparent that the peak widths are sharper for the H^+-form Nafion®, this may be attributed to adventitious water of hydration, which has been shown to plasticize PFSIs.

Conclusions

The results of this preliminary ^{19}F study show the great potential for using this technique to probe molecular relaxations in PFSIs. By examining a wider range of counterions and by increasing the temperature sampling intervals, it may be possible to pinpoint the cause of the various relaxation processes (α and β) in PFSIs.

III. PERFLUORO-ORGANIC/[INORGANIC OXIDE] NANOCOMPOSITES

A. [Perfluorosulfonate Ionomer]/[Inorganic Oxide] Nanocomposites: Organic Modification of Surfaces of *in situ* -Grown Silicon Oxide Nanoparticles

$SiO_{2[1-x/4]}(OH)_x$ nanoparticles were generated via *in situ* sol-gel reactions for tetraethoxysilane within polar clusters of perfluorosulfonic acid films. Then, residual SiOH groups on these nanoparticles were post-reacted with diethoxydimethylsilane (DEDMS) and ethoxytrimethylsilane (ETMS), resulting in organically-"shelled" and interknitted, and simply organically "shelled" nanoparticles, respectively, as shown in the following figure.

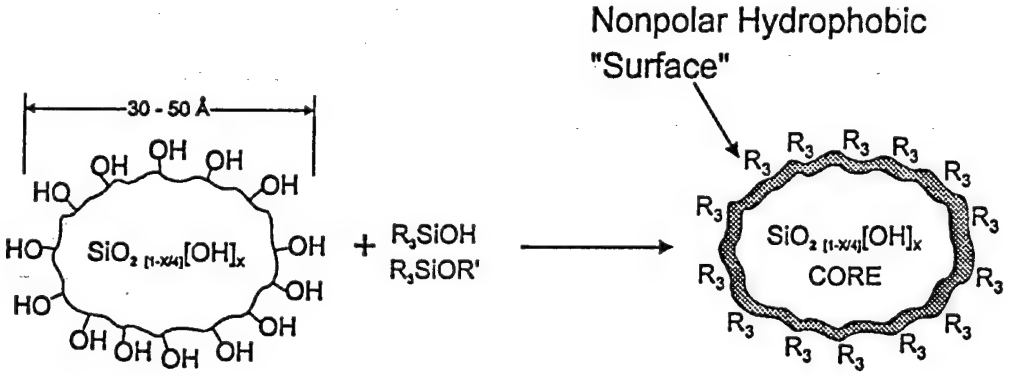

FT-IR and ^{29}Si solid state NMR spectroscopies established structural incorporation of the di- and tri-methylsilanes onto silicon oxide "cores" as well as degree of molecular connectivity within the inorganic phase. Post-reaction with DEDMS rendered the structure more linear. Mechanical tensile experiments indicated a ductile - brittle transformation upon DEDMS post-reaction, suggesting linking of silicon oxide nanoparticles. On the other hand, a measure of ductility persisted after ETMS post-reaction. Tensile strength was increased after both post-reaction schemes.

B. Novel Nafion®/ORMOSIL Hybrids via *in situ* Sol-Gel Reactions

1. *Probe of ORMOSIL Phase Nanostructures by Infrared Spectroscopy*

Novel [*Polymer*]/[*Organically-Modified Silicon Oxide* (ORMOSIL)] hybrids were formulated *via* sol-gel reactions of mixtures of tetraethoxysilane (TEOS) and diethoxydimethylsilane (DEDMS) in the nanophase-separated morphology of perfluorosulfonic acid (PFSA) films. Molecular

structures of ORMOSIL phases were investigated by FT-IR spectroscopy and the spectra compared with those of corresponding bulk ORMOSILs. Spectra are similar for PFSA-*in situ* and bulk ORMOSILs, suggesting that short range molecular structures in the two states are in fact comparable. Spectral trends with ORMOSIL composition suggest that similar D, Q sequence distributions exist for the two systems. There is evidence of co-condensation between Q and D units within the PFSA, as well as in the bulk ORMOSILs. As DEDMS:TEOS increases, ORMOSIL structures in both *in situ* and bulk states are increasingly more linear. It appears that a spectrum of energetic environment, or polarity, in the clusters of perfluorosulfonate ionomers can be tailored by adjusting the ratio of Si-OH and Si-CH_3 groups in ORMOSIL nanophases.

2. Probe of ORMOSIL Phase Nanostructure by ^{29}Si Solid State NMR Spectroscopy

[*Perfluorosulfonic Acid* (PFSA)]/[*Organically-Modified Silicon Oxide* (ORMOSIL)] hybrids were formulated *via* sol-gel reactions of mixtures of tetraethoxysilane (TEOS) and diethoxydimethylsilane (DEDMS) in the nanophase-separated morphology of a PFSA membrane (Nafion®). The molecular structures of the ORMOSIL phases were investigated by ^{29}Si solid state NMR spectroscopy and the spectra compared with those of corresponding bulk ORMOSILs. PFSA-*in situ* ORMOSIL composition can be tailored by manipulating TEOS/DEDMS source solution composition and quantified by ^{29}Si solid state NMR spectroscopy. Copolymerization of TEOS and DEDMS monomers, rather than block formation, occurs within the PFSA as well as in the bulk. As DEDMS feed concentration increases, ORMOSIL nanostructures are more hydrophobic and more flexible. Dimethylsiloxane rings are dominant in PFSAs in which hydrolysis + condensation of pure DEDMS occurs.

3. Small-Angle X-Ray Scattering Studies of Nafion®/[Silicon Oxide] and Nafion®/ORMOSIL Nanocomposites

The small angle x-ray scattering technique was used to probe structural heterogeneity on the scale of nanometers within Nafion®/[silicon oxide], Nafion®/[ORMOSIL] and Nafion®/[dimethylsiloxane] hybrid membranes. The results of this study reinforced the working hypothesis of morphological template action for the *in situ* growth of silicon oxide, or organically-modified silicon oxide phases in perfluorosulfonate ionomers *via* sol-gel reactions for silicon alkoxide or/and silicon alkylalkoxide precursors. Nanophase separation persists when incorporated silicon oxide particles are post-reacted with ethoxytrimethylsilane but post-reaction with diethoxydimethylsilane generates co-continuous phases that do not generate ionomer SAXS peaks, presumably due to a more homogeneous Si atom distribution within the ionomer. These hybrids are true nanocomposites, as structural heterogeneity exists on the scale of ~5 nm. The variation of the small angle upturn for these hybrids is explained in terms of long-range inhomogeneities in ionomers.

4. Nafion®/[Silicon Oxide] and Nafion®/ORMOSIL Hybrids via in situ Sol-Gel Reactions: Pyrene Fluorescence Probe Investigations of Nanoscale Environment

Pyrene (Py) photophysical probes were used to interrogate structural diversity within [1] Nafion®/[silicon oxide] and [2] Nafion®/[ORMOSIL] hybrids. The interior of the silicon oxide phase in [1] has the most polar environment wherein Py is trapped in silicon oxide cages in the vicinity of $-SO_3^-$ groups. Polar/nonpolar interphase regions in [1] are next in order of decreasing polarity. The interior of the ORMOSIL phase in [2] displays lowest polarity, reflecting CH_3 groups in Py-encapsulating ORMOSIL cages, and the interphase ranks somewhat higher in polarity. Water uptake is ordered: Nafion®/ORMOSIL < unfilled Nafion®-H^+ < Nafion®/[silicon oxide]. The hydrophilicity of unfilled Nafion®-H^+ is adjustable by tailoring the organic content of the incorporated sol-gel-derived nanophase as polarity determined from fluorescence emission and water uptake correlate well. Fluorescence emission of Py monitored nanostructural polarity shifts that result from secondary *in situ* gel growth induced by annealing. Additional condensation of SiOH groups and liberation of volatiles is promoted by increasing temperature/time, as evidenced by diminishing polarity. Polarity decrease with annealing is more profound for Nafion®/[ORMOSIL *incorporating Py*] than for Nafion®/[silicon oxide *incorporating Py*] as polar solvents are removed more easily from the less polar ORMOSIL nanophase.

5. Nafion®/ORMOSIL Hybrids via in situ Sol-Gel Reactions: Characterization of Fundamental Properties

Nafion®/SiO_2 and Nafion®/ORMOSIL hybrids were created via in situ sol-gel reactions for tetraethoxysilane and diethoxydimethylsilane. DSC analysis revealed that T_m for Nafion®/SiO_2 is greater than that for pure Nafion®-H^+, but decreases with progressive insertion of D units into the silicon oxide structure. A weak transition to the right of this endotherm is assigned to the melting of a minor fraction of crystallites more constrained by the filler. TGA indicates that the initial degradation step shifts to higher temperatures as D:Q increases. Dynamic mechanical spectra for Nafion®/SiO_2 shows an increase in Tg and T_m relative to Nafion®-H^+ but Tg decreases with increasing D:Q owing to increasingly flexible ORMOSIL nanostructures. Tensile strength increases and ductility decreases with decreasing D:Q. Liquid sorption experiments quantified the affinity of these hybrids for solvents of varying polarity. Membrane hydrophilicity can be tailored to be greater or less than that of pure Nafion®-H^+. Dielectric relaxation experiments revealed a major peak for Q:D = 0:1 that might be related to long range chain motions. For Q:D = 1:0, $\varepsilon'' \sim f^{-n}$ over a broad range of frequencies, which suggests intercluster proton hopping. ε' and ε'' vs. f curves reflect the flexibility of pure D structures and rigidity of pure Q structures.

6. [Perfluorosulfonate Ionomer]/ORMOSIL Nanocomposite Membranes for Gas and Liquid Permselectivity Studies

Nafion®/ORMOSIL hybrids were generated via sol-gel reactions for TEOS:diethoxydimethylsilane (DEDMS) and TEOS:triethoxyvinylsilane (TEVS) mixtures within Nafion® sulfonic acid membranes. Light microscopy verified that the sol-gel reaction did not form considerable ORMOSIL precipitates on the membrane surfaces so that the reaction product resided essentially in the membrane interior, as desired. FTIR-ATR spectroscopy established structural incorporation of the di- and tri- functional silanes into a copolymer network. In the region of the asymmetric Si-O-Si stretching vibration, the ratio of cyclic-to-linear absorbance was quantified for structural evaluation. Methyl group incorporation was observed through observation of peaks at 850 cm^{-1} and 1260 cm^{-1}. Vinyl group incorporation was observed at 3000 cm^{-1}. O-H stretching of -SiOH groups are observed at about 3500 cm^{-1}. Through increasing the relative quantity of alkyl-substituted monomers in the network, hydroxyl and cyclic peaks decrease significantly. DSC and TGA demonstrated that incorporation of these ORMOSIL networks has little effect on the thermal transitions of the polymer. ^{29}Si solid state NMR studies verified several different comonomer ratio structural uptakes. Comonomer ratio confirmation is quantitatively measured through integration of Q_4, Q_3, and Q_2 peaks. ^{13}C solid state NMR studies are in progress to attempt to determine tacticity along the polymer chain. Preliminary gas diffusion and fluorescence probe studies are in progress to examine the polarity and hydrophilicity/hydrophobicity of the internal environment of the hybrid membrane. Examination of the possibility of IPN formation through the vinyl substituent is in progress.

C. TGA-FTIR Investigation of the Thermal Degradation of Nafion®/[Silicon Oxide] Nanocomposites

Integrated TGA/FTIR studies render very significant information about the thermal degradation of unfilled Nafion®, Nafion®/SiO_2 and Nafion®/SiO_2-DEDMS-post-reacted sample. We have considered the structure variation within the ionic clusters as the invasion of sol-gel derived SiO_2 phase. Degradation mechanisms of the unfilled Nafion® and Nafion®/silica are believed to involve initial cleavage of the C-S bond leading to SO_2, OH radical, and a carbon-based radical as earlier proposed by Wilkie. In Nafion®/silica hybrid, the profound SO_2 inhibition is considered as part of sidechains immobilized within silicon oxide network "cages" that constrain reactions involving -SO_3 groups. For Nafion®/silica-PR, the decomposition process should be mainly adjusted by the post-reacted Si-CH_3 groups. TGA/FTIR is a powerful and essential tool to investigate thermal degradation in polymeric and polymer/inorganic hybrid materials.

D. Chemical Modification of a Nafion® Sulfonyl Fluoride Precursor via *in situ* Sol-Gel Reactions

The melt-processible sulfonyl fluoride precursor of a Nafion® ionomer was utilized as a sol-gel reaction medium for 3-aminopropyltriethoxysilane (APrTEOS). The diffusion-mediated reaction of APrTEOS with SO_2F groups can be controlled with high degree of reaction. FT-IR/ATR

studies show that sulfonamide linkages are formed and condensation reactions of SiOR groups provide covalent crosslinking of chains. Formic acid treatment + high temperature + long time resulted in high degree of polymer crosslinking as seen in ^{29}Si solid state NMR spectra. Mechanical modulus and strength increase, and elongation-to-break decreases with increasing filler. Hybrids with <18% uptake accumulate cracks within crosslinked outer layers, each event signaled by a drop in stress followed by stress recovery. While there are sharp visual material fronts inward from both surfaces, EDAX showed that there are no sharp Si composition boundaries. DSC revealed a broad, weak endothermic event peaking at 67 ^0C for the precursor and shifting to higher temperatures while broadening with increasing filler content, indicating progressively-restrictive T_g-related molecular motions within an increasingly nonhomogeneous environment. For the unreacted precursor, this DSC transition occurs at a temperature just above a glass transition detected by dynamic mechanical means.

E. [Perfluorosulfonate Ionomer]/[(Silicon + Metal) Oxide] Nanocomposites *via* Polymer - *in situ* Sol-Gel Chemistry

1. Nafion®/[(mixed SiO_2-TiO_2) and (mixed SiO_2-Al_2O_3)] Nanocomposites

[Mixed-metal oxide]/Nafion® hybrid films were formulated via *in situ* sol-gel reactions for tetrabutyl titanate/TEOS and for aluminum tri-*sec*-butoxide/TEOS alkoxide pairs. Inorganic composition profiles across the film thicknesses were investigated via X-ray energy dispersive spectroscopy with an environmental scanning electron microscope. Mechanical tensile analysis was used to infer [inorganic oxide]/Nafion® interfacial interactions as well as the interknitting of inorganic oxide nanoparticles. The TiO_2 component within the titaniasilicate-filled hybrids studied was concentrated in glassy near-surface regions, whereas the SiO_2-Al_2O_3 phase within aluminasilicate-filled hybrids was distributed homogeneously causing mechanical ductility. Investigations of structural topology within the inorganic oxide phases were conducted via IR and NMR spectroscopies.

2. [Nafion®]/[SiO_2-TiO_2] Nanocomposites: Sequential Alkoxide Procedure

In situ sol-gel chemistry was used to create *inorganic/perfluoro-organic* hybrids wherein titanium oxide outer regions of $SiO_{2[1\ -\ x/4]}(OH)_x$ nanoparticles, that were pre-formed in Nafion® membranes, were created by post-reaction with tetrabutyltitanate (TBT). U-shaped Si and Ti distributions across the membrane thickness direction were determined *via* x-ray energy dispersive spectroscopy. Ti/Si ratio profiles are also U-shaped, indicating more Ti relative to Si in near-surface regions. IR spectroscopy verified structural bonding of TiO_4 units onto SiO_2 nanoparticles and indicated that alkoxide hydrolysis is not complete. Reacted silicon oxide nanophases retain the topological unconnectedness possessed by the corresponding unreacted phase. IR bands signifying molecular loops and linear fragments of Si-O-Si groups are seen. ^{29}Si solid state NMR spectroscopy indicated that, for an inorganic uptake of 16.3 wt%, the Q^3 state of SiO_4 is most populated although Q^4 is only slightly less prominent and Q^2 and Q^1 are either

small or absent. The silicon oxide component, while not being predominantly linear, retains a measure of uncondensed SiOH groups. Tensile stress *vs* strain analyses suggested that TBT post-reaction links nanoparticles causing them to be contiguous over considerable distances. This percolative intergrowth occurs in near-surface regions generating a glassy zone.

F. Asymmetric Nafion®/[Zirconium Oxide] Hybrid Membranes via in situ Sol-Gel Chemistry

Nafion®-*in situ* sol-gel reactions were affected for $Zr(OBu)_4$ that permeated low water content membranes unidirectionally. IR peaks reflecting ZrO_2 and incomplete hydrolysis of ZrOBu groups near both surfaces were detected. Vibrations of $Zr(OEt)_4$ detected near both sides arise from alkoxy exchange in the presence of the solvent EtOH. Unreacted alkoxy group bands are more distinct near the non-permeated surface. An IR band for the ZnOBu group diminishes while that for ZnOEt increases with increasing time near the permeated surface due to progressive alkoxy exchange. The ZrO_2 band becomes more intense with time near the permeated surface. EDAX/SEM studies of Zr concentration across the membrane thickness verified compositional asymmetry. CO_2 gas permeability *vs* upstream pressure plots are monotonically increasing, suggesting diffusion accompanied by complex plasticization.

G. Base-Catalyzed Sol-Gel Reactions of TEOS within Nafion® Membranes

This work is similar to our previous efforts in which a silicon oxide phase was affected within Nafion® ionomers via *in situ* sol-gel reactions of TEOS. While the earlier reactions were conducted under acidic conditions, this is the first attempt using base-catalysis. Acid-catalyzed sol-gel reactions of TEOS yield primarily linear or randomly-branched structures, which as polymerization continues, entangle and form additional branches. Under base-catalysis, branched clusters form which do not interpenetrate and act as discrete, rather than open structures. These comparatively different morphologies and intramolecular connectivities within Nafion® ionomers are expected to have a dramatic effect on the physical properties of the resultant nanocomposites. In particular, we are interested in the industrially-relevant properties of gas and liquid permselectivity.

As before, we hypothesize that the quasi-ordered nanoscale morphology of Nafion® sulfonate membranes acts as a condensation polymerization template wherein the ionic clusters act as preferential sites wherein the sol-gel reaction initiates and silicon oxide nanoparticles eventually reside. Future SAXS studies of these systems will be conducted to provide verification of this hypothesis, if correct. In our experiments, TEOS is allowed to permeate membranes from external solutions for given times. Owing to the size of the clusters, we anticipate that nanoparticle dimensions will be around 30-50 Å, as in previous studies.

Several cationic forms of Nafion® are being utilized. The counterion of the $-SO_3^-$ group is always the same as the base-catalyst cation, *e.g.* $-SO_3Na^+$ and NaOH. Two categories of bases are being evaluated: (1) inorganic (Group 1 metal hydroxides (Li^+ through Cs^+) and (2) organic

(tetra-ammonium alkyl hydroxides (methyl through butyl)). Counterion radius within each base category, membrane pre-soaking with or without base, and pH are sol-gel reaction parameters that are being manipulated in these studies.

Compared with silicon oxide structures affected using acid catalysis, the structures influenced by bases are expected to have a higher degree of $Q_3 = (SiO)_3Si(OR)$ and $Q_4 = Si(OSi)_4$ Si atom coordination states at increased inorganic uptakes. This in fact has been verified using ^{29}Si solid state NMR spectroscopy in which either little or no $Q_2 = (SiO)_2Si(OR)_2$ coordination exists and Q_4 and Q_3 coordinations dominate. The network resulting from base catalysis should be more cyclic than linear in nature and this topological aspect was investigated using FTIR spectroscopy. IR bands are present that reflect SiOH network "defects" and two bands, one a signature of Si-O-Si groups in linear, and another of Si-O-Si groups in cyclic arrangements, are present. Membranes pre-soaked with base show a higher fraction of Si-O-Si groups in cycles than for those not pre-soaked with base. Additionally, base pre-soaked composites produced at higher pH values (pH>10) show more cyclic than linear Si-O-Si character.

The distribution of the silicon oxide component across the membrane thickness appears homogeneous save for at the membrane surfaces. At high uptakes (>90%) there is in fact a decrease of silicon oxide near both surfaces. At low uptakes (<10%) the opposite occurs such that more silicon oxide is at both surfaces. A profound ductile-to-brittle transformation is not expected for hybrids formulated under base catalysis owing to the discrete nature of the silicon oxide nanoparticles. Physical thermal transitions, monitored via DSC, are only slightly modified from those of a pure Nafion® control, which reinforces the previous statement. Thermodegradation (evaluated via DSC+TGA), on the other hand, is slightly retarded presumably due to silicon oxide-Nafion® template interactions. These "interactions" might consist of sidechains being trapped in the inorganic phase during the gelation process. It is expected that the relative permeabilities of gases will be different from those for composites formulated under acid-catalysis due to differences in nanoparticle porosity as well as to the lesser -SiOH content of base-catalyzed structures.

IV. REFEREED JOURNAL PUBLICATIONS RESULTING FROM THIS WORK

1. "[Perfluorosulfonate Ionomer]/[Inorganic Oxide] Nanocomposites: Organic Modification of Surfaces of *in situ*-Grown Silicon Oxide Nanoparticles", Deng, Q.; Mauritz, K.A.; Moore, R.B. in *Hybrid Organic-Inorganic Composites*, ACS Symp. Ser. 585; Mark, J.E., Bianconi, P.A., Lee, C.Y.-C., Eds., American Chemical Society: Washington D.C., 1995; Chapter 7.

2. "Novel Nafion/ORMOSIL Hybrids via in Situ Sol-Gel Reactions. 1. Probe of ORMOSIL Phase Nanostructures by Infrared Spectroscopy", Deng. Q.; Moore, R.B.; Mauritz, K.A. *Chem. Mater.* **1995**, *7* 2259.

3. "Novel Nafion/ORMOSIL Hybrids via *in Situ* Sol-Gel Reactions: 2. Probe of ORMOSIL Phase Nanostructure by ^{29}Si Solid State NMR Spectroscopy", Deng, Q.; Moore, R.B.; Jarrett, W.M.; Mauritz, K.A. *J. Sol-Gel Sci. & Technol.* In press.

4. "Small Angle X-Ray Scattering Studies of Nafion/[Silicon Oxide] and Nafion/ORMOSIL Nanocomposites", Deng, Q.; Cable, K.M.; Moore, R.B.; Mauritz, K.A. *J. Polym. Sci. B: Polym. Phys. Ed.* **1996**, *34*, ---.

5. "Nafion/ORMOSIL Hybrids via *in Situ* Sol-Gel Reactions: Pyrene Fluorescence Probe Investigations of Nanoscale Environment", Deng, Q.; Hu, Y.; Moore, R.B.; McCormick, C.L.; Mauritz,K.A. Submitted to *Chem. Mater.*

6. "[Perfluorosulfonate Ionomer]/ [Mixed Inorganic Oxide] Nanocomposites via Polymer-*in Situ* Sol-Gel Chemistry", Shao, P.L.; Mauritz, K.A.; Moore, R.B. *Chem. Mater.* **1995**, *7* 192.

7. "[Perfluorosulfonate Ionomer]/ [SiO_2-TiO_2] Nanocomposites via Polymer-*in Situ* Sol-Gel Chemistry: Sequential Alkoxide Procedure", Shao, P.L.; Mauritz, K.A.; Moore, R.B. *J. Polym. Sci. B: Phys.* **1996**, *34*, 873.

8. "Asymmetric Nafion/[Zirconium Oxide] Hybrid Membranes via in Situ Sol-Gel Chemistry", Apichatachutapan, W.; Moore, R.B.; Mauritz, K.A. *J. Appl. Polym. Sci.* **1996**. In press.

9. "Chemical Modification of a Nafion® Sulfonyl Fluoride Precursor via *in Situ* Sol-Gel Reactions", Greso, A. J.; Moore, R.B.; Cable, K.M.; Jarrett, W.L.; Mauritz, K.A. *Polymer.* In press.

10. "Anisotropic Ionic Conductivity in Uniaxially Oriented Perfluorosulfonate Ionomers", Cable, K.M.; Mauritz, K.A.; Moore, R.B. *Chem Mater.* **1995**, *7*, 1601.

11. "Effects of Hydrophilic and Hydrophobic Counterions on the Coulombic Interactions in Perfluorosulfonate Ionomers", Cable, K.M.; Mauritz, K.A.; Moore, R.B. *J. Polym. Sci. B: Phys.* **1995**, *33*, 1065.

12. "Asymmetric Nafion®/[Silicon Oxide] Hybrid Membranes via the *in Situ* Sol -Gel Reaction for Tetraethoxysilane", Gummaraju, R.V.; Moore R.B.; Mauritz, K.A. *J. Polymer Sci. B: Phys. Ed.* In press.

13. "Polyfluorinated Ionomers (Anisotropic Ionic Conductivity)," Moore, R.B.; Cable, K.M.; Mauritz, K.A. *The Polymeric Materials Encyclopedia: Synthesis, Properties and Applications*, CRC Press, Inc. In press.

V. STUDENTS AND POSTDOCTORALS INVOLVED IN THIS WORK

During the three-year period of this grant, the following students and postdoctoral associates contributed to the research effort described in this report:

Students:

Kevin M. Cable (PhD grad. stud., advisor: Moore, graduated May, 1996).
Sandra K. Young (grad. stud., advisor: Mauritz)
John P. Payne (grad. stud., advisor: Mauritz)
Wassana Apichatachutapan (undergrad. stud., advisor: Mauritz, currently PhD student, Dept. Polymer Sci., USM)

Postdoctorals:

Dr. Qin Deng, presently at Dow Corning Co., Midland MI.
Dr. Phoebe L. Shao, deceased.
Dr. Aaron G. Greso

VI. PROJECTED APPLICATIONS

It is envisioned that these, as well as similar inorganic or organically-modified inorganic nanophases can be tailored within perfluorinated ionomers, including those having carboxyate ion exchange sites, to serve as highly functional components in membranes and coatings for a number of applications. The following uses are noteworthy:

1. *Liquid-liquid separations*, in particular liquid pervaporation membrane cell technology. Our studies suggest that membranes might be nanostructured to affect solvent recovery from multicomponent solutions in industrial waste streams, or separation of organics from contaminated water, as examples.

2. *Gas separations technology* within the contexts of gas product enrichment, pollution control, and gas sensors.

Applications 1 and 2 are based on the ability to tailor the polarity and the porosity of the incorporated, sol-gel-derived nanophases.

3. The thermally-robust, high surface-to-volume, and functionalized surfaces of membrane-incorporated inorganic oxide nanoparticles can serve as platforms for the chemical attachment of catalytic metal clusters for applications within the realm of *heterogeneous catalysis*.

4. *Optical Communications*. The surfaces of inorganic oxide, or organically-modified inorganic oxide nanoparticles within these ionomers, in the form of fibers, can serve as platforms

for the attachment of molecules having nonlinear optical activity. The heterogeneities within these hybrid materials are much smaller than the wavelength of light, thereby eliminating scattering losses. Moreover, it was demonstrated that inorganic compositional gradients can be generated which would cause index of refraction gradients that could be utilized to bend light.

5. *Electrical Automobile Technology.* Fast proton-conducting membranes for fuel cells, including direct methanol cells, can be engineered by various chemical and physical modification routes. Also, advanced, high temperature high dielectric constant materials for use in capacitors to be used for surge-on-demand systems in electric automobiles are of interest.

6. Low power-consumptive, efficient membranes for *chlor-alkali cells.*

VII. REFERENCES

1. Weiss, R. A.; Agarwal, P. K.; Lundberg, R. D. *J. Appl. Polym. Sci.*, 1984, *29*, 2719.
2. Smith, P.; Eisenberg, A. *J. Polym. Sci., Polym. Phys. Ed.*, 1988, *26*, 569.
3. Hirasawa, E.; Hamazaki, H.; Tadano, K.; Yano, S. *J. Appl. Polym. Sci.*, 1991, *42*, 621.
4. Moore, R. B.; Cable, K. M.; Croley, T. L. *J. Membrane Sci.*, 1992, *75*, 7.
5. Cable, K. M.; Mauritz, K. A.; Moore, R. B. *Chem. Mater.*, 1995, *7*, 1601.
6. Kyu, T.; Eisenberg, A. in *Perfluoronated Ionomer Membranes*, Eisenberg, A.; Yeager, H. L. (eds.), ACS Symposium Series, No. 180, American Chemical Society: Washington, DC, 1982; Chapter 6.
7. Gauthier, M.; Eisenberg, A. *Macromolecules*, 1989, *22*, 3751.
8. Feldheim, D. L.; Lawson, D. R.; Martin, C. R. *J. Polym. Sci., Polym. Phys.*, 1993, *31*, 953.
9. Boyle, N. G.; McBrierty, V. J.; Douglass, D. C. *Macromolecules*, 1983, *16*, 75.
10. Boyle, N. G.; McBrierty, V. J.; Eisenberg, A. *Macromolecules*, 1983, *16*, 80.
11. Schlick, S.; Gebel, G.; Pineri, M.; Volino, F. *Macromolecules*, 1991, *24*, 3517.
12. Dec, S. F.; Wind, R. A., Maciel, G. E. *Macromolecules*, 1987, *20*, 2754.

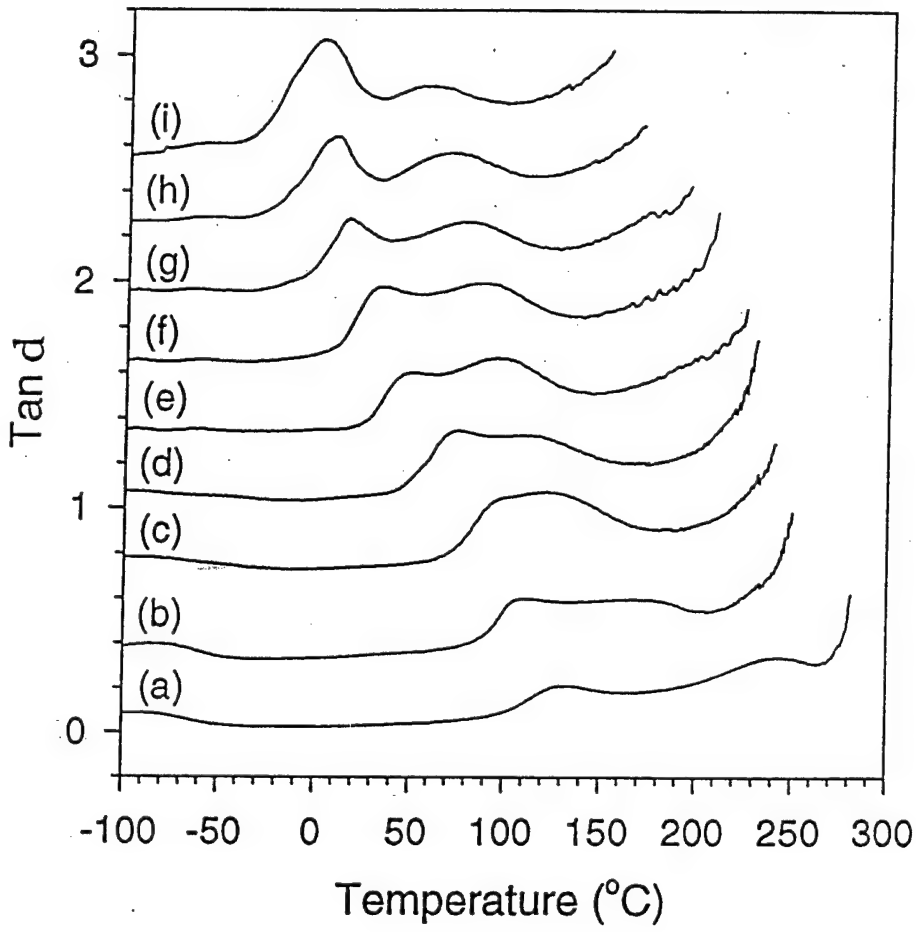

Figure 1. Tan δ plots for (a) TMA^+; (b) TEA^+; (c) TPA^+; (d) TBA^+; (e) $TPentA^+$ (f) $THexA^+$; (g) $THepA^+$; (h) $TOctA^+$; (I) $TDecA^+$ neutralized 1100 EW Nafion®.

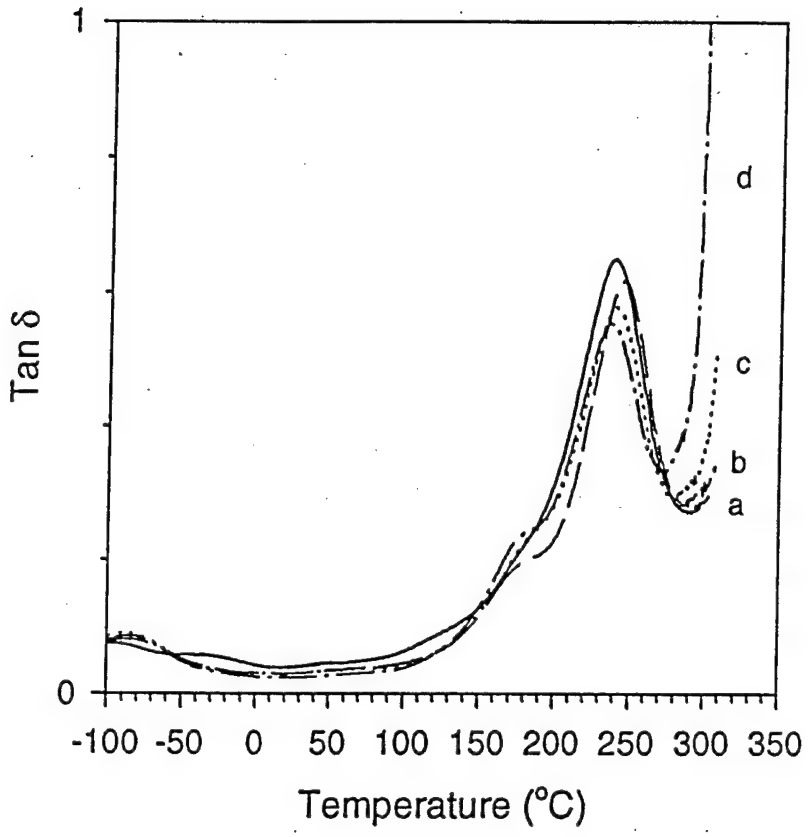

Figure 2. Tan δ plots for (a) Na^+; (b) K^+; (c) Rb^+; (d) Cs^+ neutralized 1100 EW Nafion®.

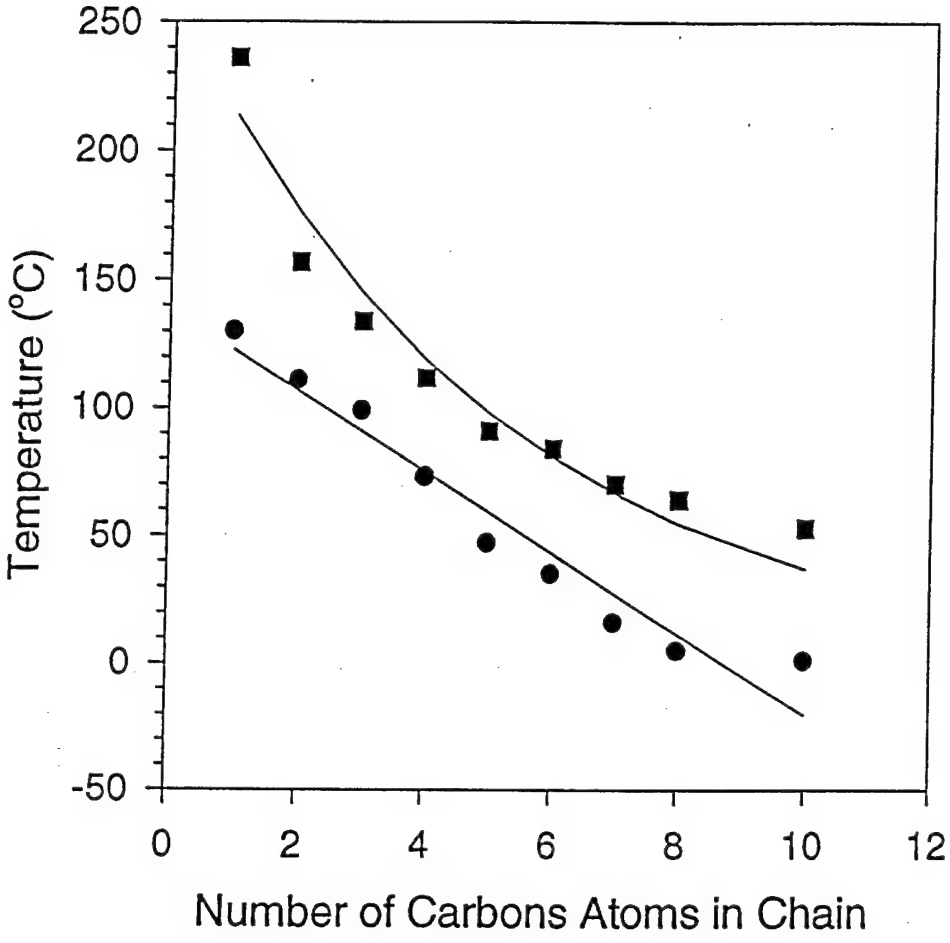

Figure 3. Plot of (■) α and (●) β relaxation temperatures versus the number of carbon atoms in the alkyl chains of the counterions.

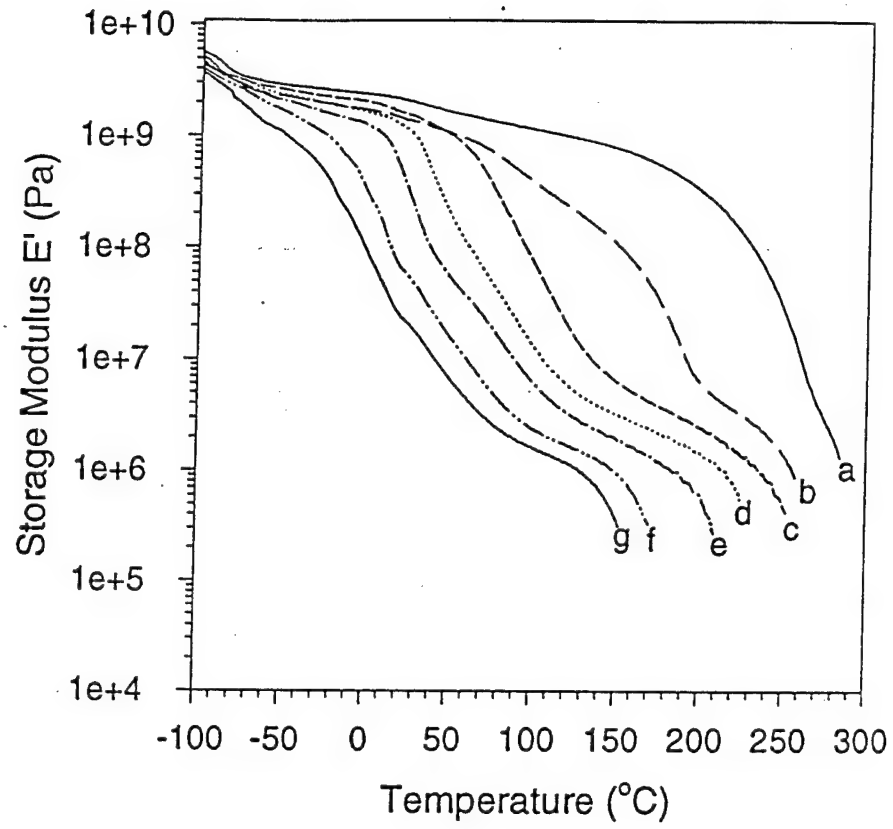

Figure 4. Storage modulus for (a) TMA^+, (b) TEA^+, (c) TPA^+, (d) $TPentA^+$, (e) $THexA^+$, (f) $TOctA^+$, and (g) $TDecA^+$ neutralized 1100 EW Nafion®.

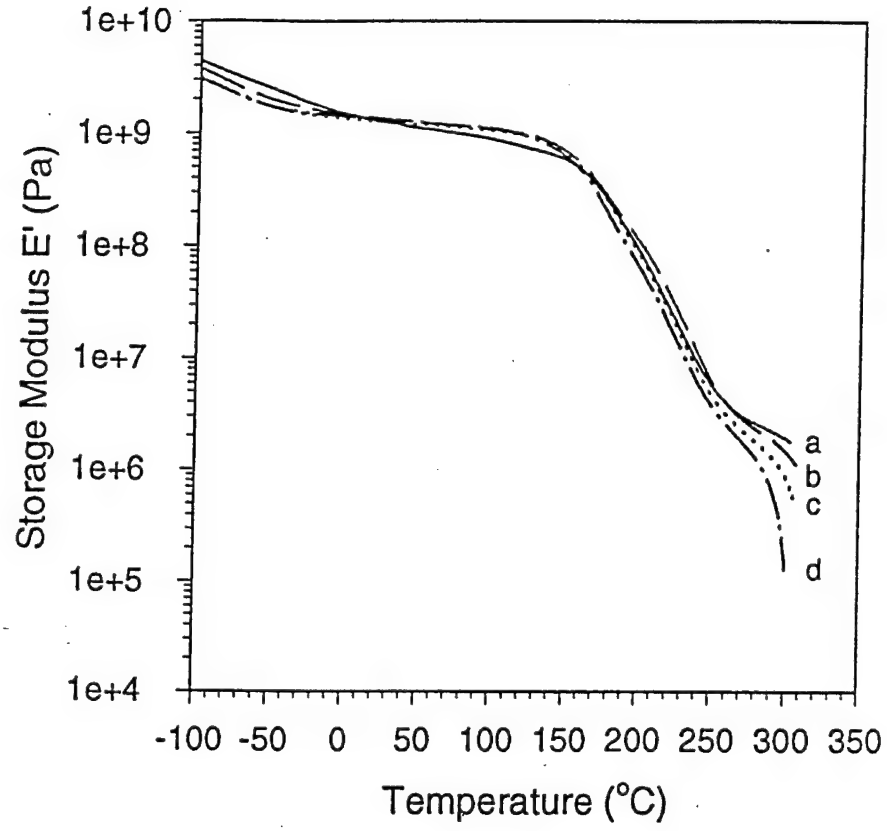

Figure 5. Storage modulus for (a) Na^+, (b) K^+, (c) Rb^+, (d) Cs^+ neutralized 1100 EW Nafion®.

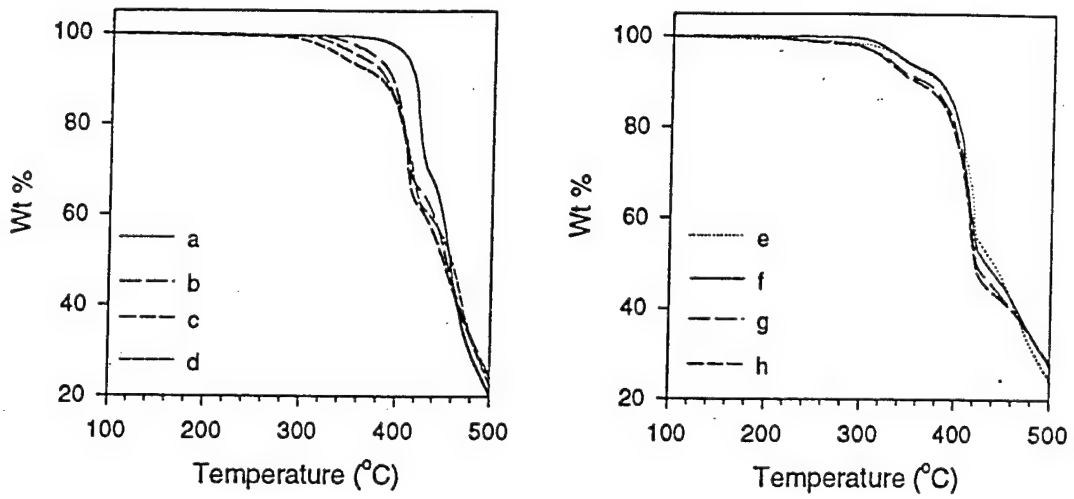

Figure 6. Thermogravimetric analysis plots for 1100 EW Nafion® neutralized with (a) TMA^+, (b) TEA^+, (c) TPA^+, (d) TBA^+, (e) $TPentA^+$,(f) $THexA^+$, (g) $THepA^+$, and (h) $TOctA^+$ counterions.

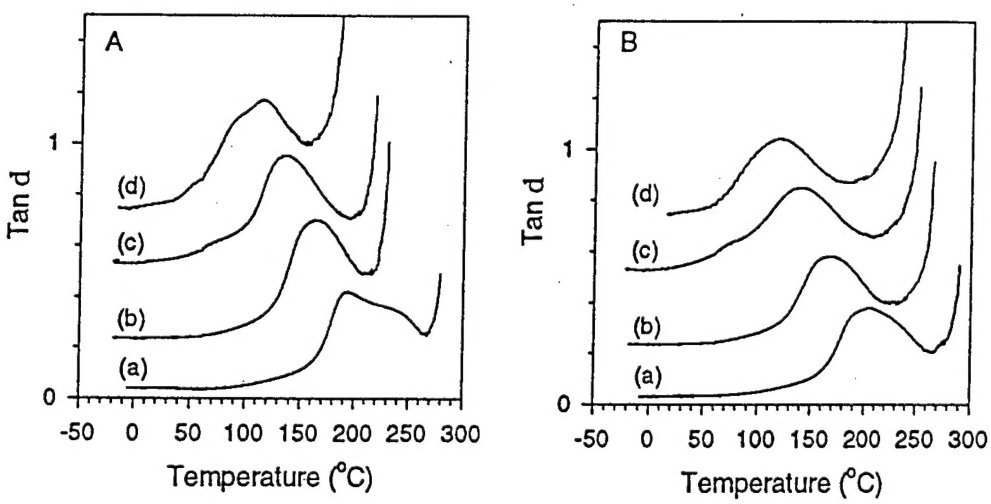

Figure 7. Tan δ plots for (A) 803 EW and (B) 1000 EW Dow PFSIs neutralized with (a) TMA^+, (b) TEA^+, (c) TPA^+, and (d) TBA^+ counterions.

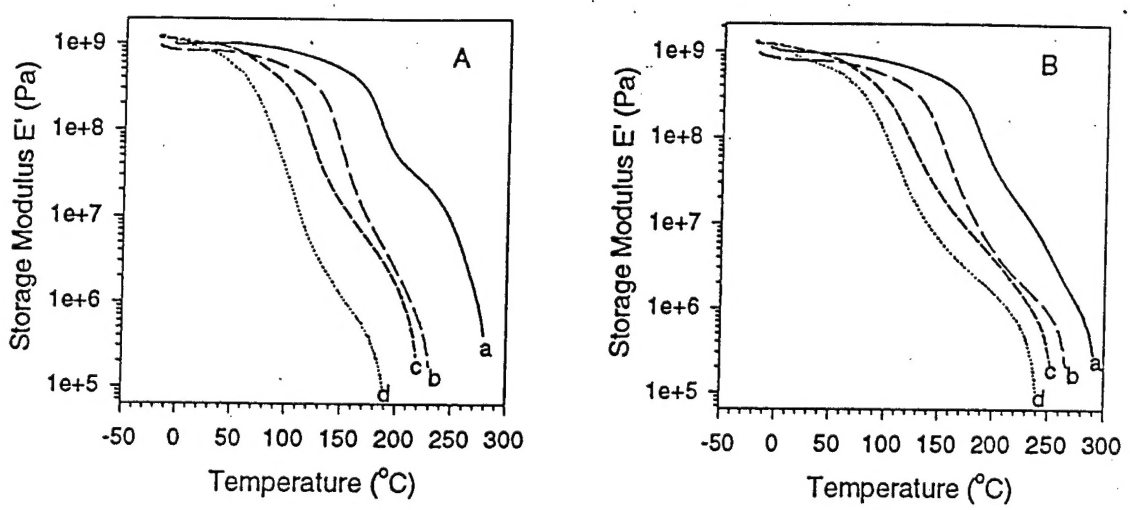

Figure 8. Storage modulus plots for (A) 803 EW and (B) 1000 EW Dow PFSIs neutralized with (a) TMA^+, (b) TEA^+, (c) TPA^+, and (d) TBA^+ counterions.

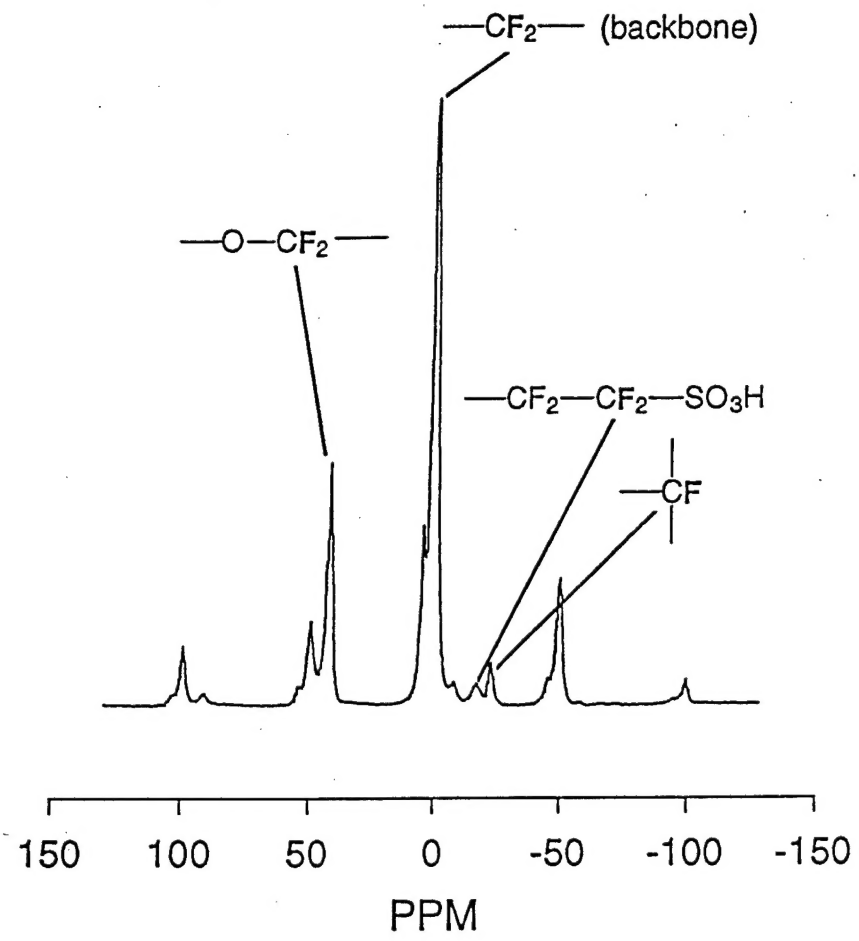

Figure 9. A typical solid-state ^{19}F spectra for H^+-form Nafion® taken at room temperature. Spectral assignments for the various peaks are depicted.

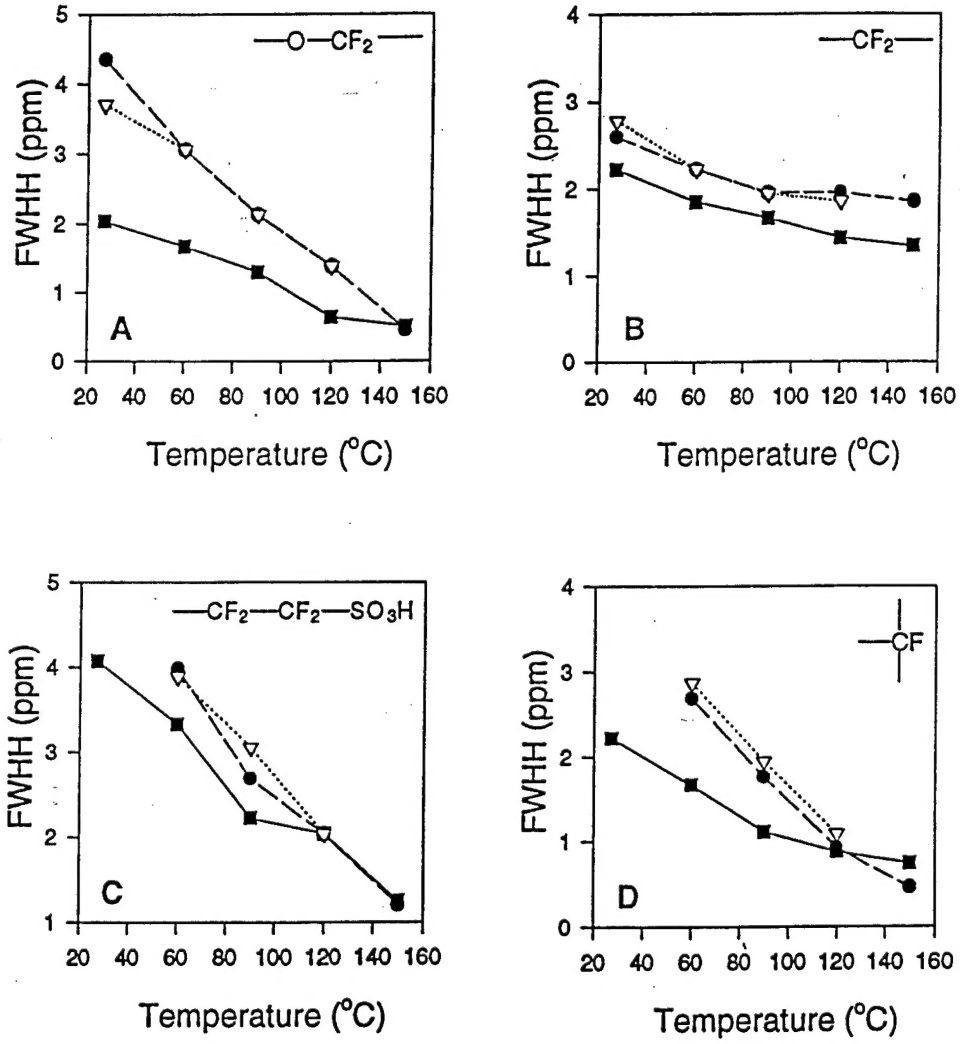

Figure 10. Graphs showing plots of full peak width at half height versus temperature for the peaks depicted in Figure IX-1. (■) H^+-form; (▼) TPA^+-form; (●) TBA^+-form.